HHS Public Access

Author manuscript

Mod Pathol. Author manuscript; available in PMC 2016 August 19.

Published in final edited form as:

Mod Pathol. 2016 April ; 29(4): 359–369. doi:10.1038/modpathol.2016.37.

The landscape of fusion transcripts in spitzoid melanoma and biologically indeterminate spitzoid tumors by RNA sequencing

Gang Wu[1], **Raymond L. Barnhill**[2], **Seungjae Lee**[3], **Yongjin Li**[1], **Ying Shao**[1], **John Easton**[1], **James Dalton**[3], **Jinghui Zhang**[1], **Alberto Pappo**[4], and **Armita Bahrami**[3]

[1]Department of Computational Biology, St. Jude Children's Research Hospital, Memphis, TN, USA

[2]Department of Pathology, Institute Curie and Faculty of Medicine, University of Paris Descartes, Paris, France

[3]Department of Pathology, St. Jude Children's Research Hospital, Memphis, TN, USA

[4]Department of Oncology, St. Jude Children's Research Hospital, Memphis, TN, USA

Abstract

Kinase activation by chromosomal translocations is a common mechanism that drives tumorigenesis in spitzoid neoplasms. To explore the landscape of fusion transcripts in these tumors, we performed whole-transcriptome sequencing using formalin-fixed paraffin-embedded tissues in malignant or biologically indeterminate spitzoid tumors from 7 patients (age 2–14 years). RNA sequence libraries enriched for coding regions were prepared and the sequencing was analyzed by a novel assembly-based algorithm designed for detecting complex fusions. In addition, tumor samples were screened for hotspot *TERT* promoter mutations, and telomerase expression was assessed by *TERT* mRNA in situ hybridization (ISH). Two patients had widespread metastasis and subsequently died of disease, and 5 patients had a benign clinical course on limited follow-up (mean: 30 months). RNA sequencing and *TERT* mRNA ISH were successful in 6 tumors and unsuccessful in 1 disseminating tumor due to low RNA quality. RNA sequencing identified a kinase fusion in 5 of the 6 sequenced tumors: *TPM3–NTRK1* (2 tumors), complex rearrangements involving *TPM3, ALK*, and *IL6R* (1 tumor), *BAIAP2L1–BRAF* (1 tumor), and *EML4–BRAF* (1 disseminating tumor). All predicted chimeric transcripts were expressed at high levels and contained the intact kinase domain. In addition, 2 tumors each contained a second fusion gene, *ARID1B-SNX9* or *PTPRZ1-NFAM1*. The detected chimeric genes were validated by home-brew break-apart or fusion fluorescence in situ hybridization. The 2 disseminating tumors each harbored the *TERT* promoter −124C>T (Chr 5:1,295,228 hg19 coordinate) mutation whereas the remaining 5 tumors retained the wild-type gene. The presence of the −124C>T mutation correlated with telomerase expression by *TERT* mRNA ISH. In summary,

Correspondence: Armita Bahrami, M.D., Department of Pathology, St. Jude Children's Research Hospital, 262 Danny Thomas Place, Memphis, TN, 38105-3678, USA, Phone: (901) 595-7116, ; Email: armita.bahrami@stjude.org

This work was presented in part at the 2015 United States and Canadian Academy of Pathology Annual Meeting in Boston, MA.

Disclosure/Conflict of Interest: The authors declare no conflict of interest.

we demonstrated complex fusion transcripts and novel partner genes for *BRAF* by RNA sequencing of FFPE samples. The diversity of gene fusions demonstrated by RNA sequencing defines the molecular heterogeneity of spitzoid neoplasms.

Keywords

RNA sequencing; kinase fusion; Spitz tumor; spitzoid melanoma

INTRODUCTION

Spitzoid tumors are a clinicopathologically distinct class of melanocytic neoplasms that occur more commonly in younger individuals and account for the majority of so-called “melanomas” seen in the pediatric population. Histologically, these lesions are characterized by compound or dermal proliferations of large epithelioid and/or spindle-shaped melanocytes having abundant eosinophilic cytoplasm, often forming junctional nests in conjunction with epidermal hyperplasia. The lack of objective criteria to determine the malignant potential of spitzoid tumors is a major diagnostic challenge.[1–5] The established histopathologic criteria used to differentiate nevi from conventional melanoma are not reliable for spitzoid neoplasms. Also, unlike conventional melanoma, lymph node metastasis in general is not predictive of poor clinical outcome in patients with spitzoid tumors.[6–13]

Spitzoid lesions with features significantly deviating from a stereotypical Spitz nevus, such as large lesional size (>1 cm), asymmetry, ulceration, pagetoid melanocytosis extending peripherally, significant intradermal mitotic activity, lack of cellular maturation with depth, confluent cellular growth, involvement of subcutaneous fat, or severe cytologic atypia, are considered atypical spitzoid melanocytic proliferations, encompassing atypical Spitz tumor and spitzoid melanoma. Additional important clinical information includes the age of the patient, since melanoma is extremely rare under the age of 10 years, and clinical features such as a new or rapidly-growing lesion, asymmetry, irregular coloration, ulceration, bleeding, and history of trauma. The diagnosis of spitzoid melanoma in these circumstances is considered when multiple chromosomal aberrations are detected by using ancillary molecular techniques, such as the multiprobe fluorescent in situ hybridization (FISH) assay[14, 15] or comparative genomic hybridization analysis.[16, 17] The true predictive value of these assays for determining clinical outcome in spitzoid tumors, however, remains uncertain. We recently evaluated 56 spitzoid tumors for the presence of telomerase reverse transcriptase (*TERT)* promoter mutations and their association with disease progression. We found a hotspot *TERT* promoter mutation in tumors from patients who had a malignant clinical course but not in tumors from patients who had a favorable clinical outcome, which suggests that these mutations contribute to malignant biological behavior.[12] Nonetheless, the underlying molecular mechanisms responsible for the potential of these lesions to spread distantly need to be investigated further.

The Cancer Genome Atlas Network has recently proposed a genomic classification of cutaneous melanomas into 4 mutually exclusive genetic subtypes on the basis of the presence of a hotspot mutation in the significantly mutated melanoma-associated genes,

BRAF, RAS (*N/K/H*), *NF1*, and the triple wild-type.[18] By this stratification scheme, most spitzoid melanomas are likely to fall into the triple wild-type subtype,[19, 20] a heterogeneous molecular category shown to be enriched by focal amplifications or complex structural rearrangements.[18] Wiesner et al. and others demonstrated that instead of activation of the MAP kinase pathway through point mutations, chromosomal translocations-induced kinase fusions drive tumorigenesis in spitzoid neoplasms.[21–24] These rearrangements are predicted to constitutively activate the MAP kinase pathway by an in-frame fusion of the receptor tyrosine kinase *NTRK1, ROS1, RET, ALK*, or *MET* or the serine/threonine kinase *BRAF* to the N terminal of various 5 partner genes.[21, 23, 24] Since these genetic alterations are present in the entire biologic spectrum of the disease, that is, the benign (nevi), the biologically indeterminate or low-grade malignant (atypical Spitz tumors), and the overtly malignant lesions (spitzoid melanoma), they are likely acquired in the early stage of disease but cannot by themselves lead to melanoma.[25, 26]

To explore the landscape of structural rearrangements in spitzoid melanomas, in the current study we used RNA sequencing to characterize the transcriptome of 7 histologically malignant or biologically indeterminate spitzoid tumors. Furthermore, we used *TERT* mRNA in situ hybridization (ISH) to demonstrate the association between *TERT* promoter mutations and telomerase expression at the cellular level.

MATERIALS AND METHODS

Study Population

The study was approved by the institutional review boards of participating institutions. The study subjects were selected from a previously reported cohort of 56 patients with spitzoid melanocytic tumors[12] for whom documented clinical outcomes and sufficient biological material were available. To improve the performance of RNA sequencing, only biological samples with a storage time of =<7 years were considered for the study. As an exception, an old archived formalin-fixed paraffin-embedded (FFPE) block (>20 years old) from a rare fatal spitzoid melanoma in a young patient was also included. Adequate biologic material was obtained for RNA sequencing from 7 malignant or biologically indeterminate spitzoid tumors (5 primary tumors and 2 metastatic tumors).

The hotspot *BRAF, NRAS*, and *TERT* promoter mutation data on these tumors have been previously reported.[12] In summary, genomic DNA was extracted from the tumor samples (5 primary tumors, 1 paired primary and metastatic tumor, and 1 metastatic tumor) and screened for hotspot mutations of the genes by PCR and Sanger sequencing, as previously described.[20]

Transcriptome Sequencing

Tumor tissue samples from 8–10 FFPE slide-mounted sections were manually dissected, with corresponding H&E sections used to guide dissections, to obtain at least 70% tumor purity. RNA was isolated by using the Maxwell system (Promega). RNA was quantitated by fluorescence dye staining by using the Quant-iT (Life Technologies) RNA assay. RNA quality was evaluated by using a 2100 Bioanalyzer (Agilent Technologies) with a Nano

RNA 6000 Chip. RNASEQ libraries enriched for coding regions were prepared by using the Truseq RNA Access Library Prep Kit (Illumina), following the manufacturer's protocol for RNA input quantity relative to RNA quality. Sequencing was performed on HiSeq2000 (Illumina) to generate 100-bp paired-end reads.

RNA Sequencing Analysis

RNA sequencing data were generated as previously described.[25] Paired-end reads from RNA sequences were aligned to the following 4 database files by using BWA (0.5.10) aligner: (1) the human GRCh37-lite reference sequence, (2) RefSeq, (3) a sequence file representing all possible combinations of non-sequential pairs in RefSeq exons, and (4) an AceView database flat file downloaded from UCSC, which represents transcripts constructed from human expressed sequence tags. The mapping results from files (2), (3), and (4) were aligned to human reference genome coordinates and also to the human GRCh37-lite reference sequence by using STAR 2.3.0 without annotations. The final BAM file was constructed by selecting the best alignment among the 5 mappings. The coverage was calculated by using an in-house pipeline. Structural variations were detected by using CICERO, a novel algorithm that uses de novo assembly to identify structural variations in RNA sequences.

Fluorescence In Situ Hybridization

BAC clones (BACPAC Resources) were used to develop break-apart probes for the following genes: *BRAF* (RP11-837G3, RP11-948O19), *NTRK1* (CH17-67O18, RP11-1038N13), *PTPRZ1* (CH17-132B19, RP11-99L10), *IL6R* (CH17-169C19, RP11-627K14), *TPM3* (CH17-317C21, CH17-169C19), *EML4* (CH17-315G08, RP11-885P15), *ARID1B* (RP11-230C9, CH17-280H05), and *BAIAP2L1* (RP11-958G24, CH17-112O19). Break-apart FISH for *ALK* was performed by using a commercially available probe set (CytoCell, Cat# LPS 019-A). In addition, BAC clones (CH17-132B19, RP11-99L10 and CH17-57M15, CH17-240N01) were used to develop a fusion probe set for *PTPRZ1–NFAM1*. Dual-color FISH was performed on 4-μm FFPE sections, as previously described.[20]

TERT mRNA In Situ Hybridization

mRNA ISH, a novel method to detect mRNA in FFPE tissues,[26] was performed for *TERT* mRNA on a Discovery Ultra automation system (Ventana Medical Systems, Inc.) by using RNAscope® VS Reagent Kit – RED (Advanced Cell Diagnostics). VS Probe – Hs-*TERT* (Cat#605516) specific to the sequence region between nucleotides 2164 to 3231 encoding the *TERT* transcript was used according to the manufacturer's instructions. Briefly, 4-μm FFPE tissue sections of tumors were pretreated in citrate buffer with heat, followed by protease digestion before hybridization with the target oligo probes. Slides were hybridized sequentially with target probes incubated at 43°C for 2 h and 32 min, preamplifier at 53°C for 32 min, and amplifier at 53°C for 32 min, and label probes at room temperature for 12 min. Between the hybridization steps, slides were washed with Ribowash buffer (0.1× saline sodium citrate). Hybridization signals were detected by chromogenic development with Fast Red, followed by counterstaining with hematoxylin. Each sample was quality controlled for RNA integrity with an RNAscope probe for PPIB RNA and for background with a probe for

bacterial dapB RNA. The specific RNA staining signal was identified as intracellular red punctate dots.

RESULTS

Clinicopathologic Findings

Table 1 and Figures 1–5 show the clinical and disease characteristics for the 7 patients. Tumors were detected in samples from 4 children (age 2–7 years) and 3 adolescents (age 11–14 years) and involved the lower extremities (n=5), ear (n=1), and trunk (n=1). Two patients had clinically detectable lymphadenopathy (macrometastasis). Of 6 patients whose sentinel/regional lymph nodes were examined, 5 patients were positive for nodal metastasis (Table 1), with clinically detectable lymphadenopathy (*patients 5 and 7*), large nodal deposits (*patients 2 and 3*), and isolated tumor cells (*patient 1*). At a median follow-up of 20 months (range, 6–72 months), 5 patients were alive and well with no evidence of disease and 2 patients developed distant metastasis in the lungs and brain and subsequently succumbed to the disease 18 and 24 months after diagnosis (Table 1).

BRAF, NRAS, and *TERT* promoter Mutations

The 7 spitzoid tumors were negative for the activating point mutations in *BRAF* and *NRAS*. The 2 tumors that led to a fatal outcome each harbored a *TERT* promoter mutation at −124 bp from the ATG start site (−124C>T) in the primary and metastatic samples whereas the 5 other tumors retained the *TERT* promoter wild-type (Table 1).

Fusion Transcripts by RNA sequencing

RNA sequencing was successful in 6 of the 7 samples, with a minimum 20× coverage of at least 20% exonic bases and a median coverage of 10× in all RefSeq annotated exons (Supplementary Table 1). Coverage was low in 1 sample obtained from old FFPE material (*patient 7*), and it was excluded from analysis. RNA sequencing identified a kinase fusion in 5 of the 6 successfully tested tumors (Supplementary Table 2). The following fusion genes were identified by RNA sequencing: *EML4–BRAF* (1 disseminating tumor; Figure 1), *BAIAP2L1–BRAF* (1 tumor; Figure 2), *TPM3–NTRK1* (2 tumors; Figure 3), and *TPM3–ALK* (1 tumor; Figure 4). All predicted chimeric transcripts were expressed at high levels and contained the intact kinase domain. The FPKM (fragment per kilobase per million mapped reads) expression values for the fusion genes are provided in Table 2 Supplement. In addition, 2 spitzoid tumors each carried a second fusion gene, *ARID1B–SNX9* and *PTPRZ1–NFAM1* (Supplementary Figure 1). There was no structural rearrangement in 1 of the successfully sequenced samples (*patient 6*).

Fluorescence In Situ Hybridization

Break-apart FISH for *BRAF* (2 tumors), *NTRK1* (2 tumors), *PTPRZ1* (1 tumor), *IL6R* (1 tumor), *TPM3* (3 tumors), *EML4* (1 tumor), *ARID1B* (1 tumor), and *BAIAP2L1* (1 tumor) showed split signals in at least 30% of the evaluated cells, which indicated rearrangement of the respective genes (Figures 1–4 and Supplementary Figure 1). The *PTPRZ1–NFAM1* fusion FISH showed multiple copies of overlapping signals (Supplementary Figure 1), which suggested gene fusion followed by copy gain in the kinase fusion gene.

TERT mRNA In Situ Hybridization

TERT mRNA ISH showed distinct bright intracellular signals in melanocytes in the *TERT* promoter mutant metastasizing tumor (Figure 1) but not in the wild-type *TERT* promoter tumors (Figure 2). *TERT* mRNA ISH was not successful in 1 sample (*patient 7*) because of low RNA quality.

DISCUSSION

By using RNA sequencing, we identified in-frame fusions of kinases, *BRAF, NTRK1*, and *ALK*, in a mutually exclusive pattern, with various partner genes in 5 of the 6 successfully sequenced spitzoid tumors. We found 2 novel 5 *BRAF* fusion partners *EML4* and *BAIAP2L1*, which expands the list of BRAF N-terminal fusion partners previously described in pilocytic astrocytoma and melanocytic tumors.[21–23, 27] *EML4* is a recurrent fusion partner gene with *ALK*, and the resulting fusion transcript *EML4–ALK* is the primary oncogenic driver in 3%–6% of non-small-cell lung carcinomas.[28, 29] However, to our knowledge, there are no reports of *EML4* participating in an oncogenic fusion with *BRAF*. *BAIAP2L1* (*BAI1-associated protein 2-like 1*) has been reported to participate in the fusion transcript with *FGFR3* in bladder and lung cancer, but never described previously in melanoma.[30–32]

One of the samples in our study (*patient 4*) harbored the *TPM3–ALK* fusion, which has been previously reported in spitzoid neoplasms.[33, 34] Interestingly, before the discovery of its oncogenic association with melanocytic neoplasms, *TPM3–ALK* was identified in tumors from other lines of differentiation, namely the mesenchymal (inflammatory myofibroblastic tumor),[35] the lymphoid (anaplastic large-cell lymphoma)[36], and the epithelial (squamous cell carcinoma and renal cancer) lineages.[37, 38] This finding supports the assertion that known fusion genes can drive oncogenesis in tumors of different cell types. In addition to translocations, ALK is also activated through a de novo alternative transcription initiation, without genetic alterations at the *ALK* locus, in approximately 11% of melanomas.[39]

Certain morphologic features have been linked to spitzoid tumors with *ALK* rearrangement.[24, 34] Similar features were seen in our patient sample with *ALK* fusion that exhibited nests of spindle shaped melanocytes with fascicular infiltration of the dermis and subcutis (Figure 4). Although no definitive conclusions can be drawn because of the small number of samples in this study, the 2 samples with *NTRK1* fusion shared a few morphologic features such as prominent cellularity, deep extension, nested arrangement in the upper part, and confluent cellular nodules with rounded pushing margins at the bottom (Figure 3). How reliably these morphologic manifestations predict the type of fusion transcripts has not yet been sufficiently studied. In any case, given the diversity of gene fusions involving alternative partners or even alternative exons within the same pairs of genes, as demonstrated in 2 spitzoid melanomas in this series harboring *TMP3-NTRK1* (Figure 3), or other coexisting genetic alterations, the morphologic heterogeneity in spitzoid tumors even with the same kinase fusion is not unexpected.

Of the 2 patients with fatal outcomes in our study, one carried a *BRAF* fusion and the sample from the other patient could not be successfully sequenced due to degraded RNA.

The second patient with *BRAF* fusion in our series had a benign course of disease. To date, the association between the type of fusion gene and prognosis in patients with spitzoid tumors remains uncertain. Tumors from both patients with fatal outcomes harbored the −124C>T transcriptional activating mutation in the *TERT* promoter. The −124C>T mutation (also referred to as C228T in the literature) has been previously shown to correlate with high *TERT* mRNA expression in melanoma,[18] and here on a different platform using *TERT* mRNA ISH, we demonstrated its association with telomerase expression at a cellular level (Figure 1).

Transcriptome sequencing identified additional novel fusion genes accompanied with kinase fusions in spitzoid tumors. One sample harbored the *PTPRZ1–NFAM1*, which was associated with elevated expression of the *NFAT activated protein with ITAM motif 1* (*NFAM1*) (FPKM= 621.2). The protein encoded by *NFAM1* contains an immunoreceptor tyrosine-based activation motif that is thought to regulate the development of B cells,[40] but its role in cancer development and melanoma is not well studied. The 5 partner gene *PTPRZ1* is a recurrent fusion partner with *MET* in glioblastoma.[41] The fusion transcript *ARID1B–SNX9* is expected to lead to the loss of function of the tumor suppressor gene *ARID1B*, which is a subunit of the SWI/SNF complex. Although the exact function of *ARID1B* in melanoma has not been investigated, 13% of melanomas have a loss-of-function mutation in a component of the SWI/SNF complex,[42] suggesting that the chromatin remodeling complex plays a role in melanoma tumorigenesis. Although the oncogenic contribution of these genetic alterations remains speculative until they are functionally characterized, our findings, together with the complex nature of translocation events seen in the tumor samples, suggest that spitzoid tumors are enriched with structural rearrangements.

Notably, no structural rearrangement was identified in 1 spitzoid tumor in our study (Table 1; *patient 6*), even though the exonic coverage for this sample was comparable to that of other specimens (Supplementary Table 1). Therefore, we speculate that in a subset of spitzoid neoplasms, mechanisms other than translocations can activate oncogenes. Whole-genome sequencing can give further insights into the oncogenic mechanisms of these tumors.

In summary, we demonstrate complex and heterogeneous structural rearrangements in spitzoid tumors by transcriptome sequencing by using FFPE tissue. The heterogeneity of the fusion transcripts observed by RNA sequencing correlates with the morphologic and clinical diversity of this group of melanocytic tumors. The association between *TERT* promoter mutations or telomerase expression with outcomes in patients with spitzoid melanocytic tumors requires further studies.

Supplementary Material

Refer to Web version on PubMed Central for supplementary material.

Acknowledgments

This study was supported in part by the National Cancer Institute of the National Institutes of Health under Award Number P30CA021765 and by ALSAC.

References

1. Reed D, Kudchadkar R, Zager JS, Sondak VK, Messina JL. Controversies in the evaluation and management of atypical melanocytic proliferations in children, adolescents, and young adults. J Natl Compr Canc Netw. 2013; 11:679–686. [PubMed: 23744867]
2. Barnhill RL, Argenyi ZB, From L, et al. Atypical Spitz nevi/tumors: lack of consensus for diagnosis, discrimination from melanoma, and prediction of outcome. Hum Pathol. 1999; 30:513–520. [PubMed: 10333219]
3. Gerami P, Busam K, Cochran A, et al. Histomorphologic assessment and interobserver diagnostic reproducibility of atypical spitzoid melanocytic neoplasms with long-term follow-up. Am J Surg Pathol. 2014; 38:934–940. [PubMed: 24618612]
4. Spatz A, Barnhill RL. The Spitz tumor 50 years later: revisiting a landmark contribution and unresolved controversy. J Am Acad Dermatol. 1999; 40:223–228. [PubMed: 10025749]
5. Cerroni L, Barnhill R, Elder D, et al. Melanocytic tumors of uncertain malignant potential: results of a tutorial held at the XXIX Symposium of the International Society of Dermatopathology in Graz, October 2008. Am J Surg Pathol. 2010; 34:314–326. [PubMed: 20118771]
6. Paradela S, Fonseca E, Pita S, et al. Spitzoid melanoma in children: clinicopathological study and application of immunohistochemistry as an adjunct diagnostic tool. J Cutan Pathol. 2009; 36:740–752. [PubMed: 19032380]
7. Berk DR, LaBuz E, Dadras SS, Johnson DL, Swetter SM. Melanoma and melanocytic tumors of uncertain malignant potential in children, adolescents and young adults--the Stanford experience 1995–2008. Pediatr Dermatol. 2010; 27:244–254. [PubMed: 20403119]
8. Busam KJ, Pulitzer M. Sentinel lymph node biopsy for patients with diagnostically controversial Spitzoid melanocytic tumors? Adv Anat Pathol. 2008; 15:253–262. [PubMed: 18724099]
9. Hung T, Piris A, Lobo A, et al. Sentinel lymph node metastasis is not predictive of poor outcome in patients with problematic spitzoid melanocytic tumors. Hum Pathol. 2013; 44:87–94. [PubMed: 22939951]
10. Ludgate MW, Fullen DR, Lee J, et al. The atypical Spitz tumor of uncertain biologic potential: a series of 67 patients from a single institution. Cancer. 2009; 115:631–641. [PubMed: 19123453]
11. Lallas A, Kyrgidis A, Ferrara G, et al. Atypical Spitz tumours and sentinel lymph node biopsy: a systematic review. Lancet Oncol. 2014; 15:e178–e183. [PubMed: 24694641]
12. Lee S, Barnhill RL, Dummer R, et al. TERT Promoter Mutations Are Predictive of Aggressive Clinical Behavior in Patients with Spitzoid Melanocytic Neoplasms. Sci Rep. 2015; 5:11200. [PubMed: 26061100]
13. Busam KJ, Murali R, Pulitzer M, et al. Atypical spitzoid melanocytic tumors with positive sentinel lymph nodes in children and teenagers, and comparison with histologically unambiguous and lethal melanomas. Am J Surg Pathol. 2009; 33:1386–1395. [PubMed: 19609204]
14. Gerami P, Zembowicz A. Update on fluorescence in situ hybridization in melanoma: state of the art. Arch Pathol Lab Med. 2011; 135:830–837. [PubMed: 21732770]
15. Gerami P, Scolyer RA, Xu X, et al. Risk assessment for atypical spitzoid melanocytic neoplasms using FISH to identify chromosomal copy number aberrations. Am J Surg Pathol. 2013; 37:676–684. [PubMed: 23388126]
16. Bastian BC, Olshen AB, LeBoit PE, Pinkel D. Classifying melanocytic tumors based on DNA copy number changes. Am J Pathol. 2003; 163:1765–1770. [PubMed: 14578177]
17. Ali L, Helm T, Cheney R, et al. Correlating array comparative genomic hybridization findings with histology and outcome in spitzoid melanocytic neoplasms. Int J Clin Exp Pathol. 2010; 3:593–599. [PubMed: 20661407]
18. Genomic Classification of Cutaneous Melanoma. Cell. 2015; 161:1681–1696. [PubMed: 26091043]
19. Yazdan P, Cooper C, Sholl LM, et al. Comparative analysis of atypical spitz tumors with heterozygous versus homozygous 9p21 deletions for clinical outcomes, histomorphology, BRAF mutation, and p16 expression. Am J Surg Pathol. 2014; 38:638–645. [PubMed: 24451276]
20. Lu C, Zhang J, Nagahawatte P, et al. The genomic landscape of childhood and adolescent melanoma. J Invest Dermatol. 2015; 135:816–823. [PubMed: 25268584]

21. Wiesner T, He J, Yelensky R, et al. Kinase fusions are frequent in Spitz tumours and spitzoid melanomas. Nature communications. 2014; 5:3116.
22. Hutchinson KE, Lipson D, Stephens PJ, et al. BRAF fusions define a distinct molecular subset of melanomas with potential sensitivity to MEK inhibition. Clin Cancer Res. 2013; 19:6696–6702. [PubMed: 24345920]
23. Botton T, Yeh I, Nelson T, et al. Recurrent BRAF kinase fusions in melanocytic tumors offer an opportunity for targeted therapy. Pigment Cell Melanoma Res. 2013; 26:845–851. [PubMed: 23890088]
24. Yeh I, Botton T, Talevich E, et al. Activating MET kinase rearrangements in melanoma and Spitz tumours. Nature communications. 2015; 6:7174.
25. Parker M, Mohankumar KM, Punchihewa C, et al. C11orf95-RELA fusions drive oncogenic NF-kappaB signalling in ependymoma. Nature. 2014; 506:451–455. [PubMed: 24553141]
26. Wang F, Flanagan J, Su N, et al. RNAscope: a novel in situ RNA analysis platform for formalin-fixed, paraffin-embedded tissues. J Mol Diagn. 2012; 14:22–29. [PubMed: 22166544]
27. Jones DT, Kocialkowski S, Liu L, et al. Tandem duplication producing a novel oncogenic BRAF fusion gene defines the majority of pilocytic astrocytomas. Cancer Res. 2008; 68:8673–8677. [PubMed: 18974108]
28. Kwak EL, Bang YJ, Camidge DR, et al. Anaplastic lymphoma kinase inhibition in non-small-cell lung cancer. N Engl J Med. 2010; 363:1693–1703. [PubMed: 20979469]
29. Takeuchi K, Choi YL, Soda M, et al. Multiplex reverse transcription-PCR screening for EML4-ALK fusion transcripts. Clin Cancer Res. 2008; 14:6618–6624. [PubMed: 18927303]
30. Williams SV, Hurst CD, Knowles MA. Oncogenic FGFR3 gene fusions in bladder cancer. Hum Mol Genet. 2013; 22:795–803. [PubMed: 23175443]
31. Nakanishi Y, Akiyama N, Tsukaguchi T, et al. Mechanism of Oncogenic Signal Activation by the Novel Fusion Kinase FGFR3-BAIAP2L1. Mol Cancer Ther. 2015; 14:704–712. [PubMed: 25589496]
32. Shinmura K, Kato H, Matsuura S, et al. A novel somatic FGFR3 mutation in primary lung cancer. Oncol Rep. 2014; 31:1219–1224. [PubMed: 24452392]
33. Yeh I, de la Fouchardiere A, Pissaloux D, et al. Clinical, histopathologic, and genomic features of Spitz tumors with ALK fusions. Am J Surg Pathol. 2015; 39:581–591. [PubMed: 25602801]
34. Busam KJ, Kutzner H, Cerroni L, Wiesner T. Clinical and pathologic findings of Spitz nevi and atypical Spitz tumors with ALK fusions. Am J Surg Pathol. 2014; 38:925–933. [PubMed: 24698967]
35. Lawrence B, Perez-Atayde A, Hibbard MK, et al. TPM3-ALK and TPM4-ALK oncogenes in inflammatory myofibroblastic tumors. Am J Pathol. 2000; 157:377–384. [PubMed: 10934142]
36. Lamant L, Dastugue N, Pulford K, Delsol G, Mariame B. A new fusion gene TPM3-ALK in anaplastic large cell lymphoma created by a (1;2)(q25;p23) translocation. Blood. 1999; 93:3088–3095. [PubMed: 10216106]
37. Jazii FR, Najafi Z, Malekzadeh R, et al. Identification of squamous cell carcinoma associated proteins by proteomics and loss of beta tropomyosin expression in esophageal cancer. World J Gastroenterol. 2006; 12:7104–7112. [PubMed: 17131471]
38. Sugawara E, Togashi Y, Kuroda N, et al. Identification of anaplastic lymphoma kinase fusions in renal cancer: large-scale immunohistochemical screening by the intercalated antibody-enhanced polymer method. Cancer. 2012; 118:4427–4436. [PubMed: 22252991]
39. Wiesner T, Lee W, Obenauf AC, et al. Alternative transcription initiation leads to expression of a novel ALK isoform in cancer. Nature. 2015; 526:453–457. [PubMed: 26444240]
40. Ohtsuka M, Arase H, Takeuchi A, et al. NFAM1, an immunoreceptor tyrosine-based activation motif-bearing molecule that regulates B cell development and signaling. Proc Natl Acad Sci U S A. 2004; 101:8126–8131. [PubMed: 15143214]
41. Bao ZS, Chen HM, Yang MY, et al. RNA-seq of 272 gliomas revealed a novel, recurrent PTPRZ1-MET fusion transcript in secondary glioblastomas. Genome Res. 2014; 24:1765–1773. [PubMed: 25135958]
42. Hodis E, Watson IR, Kryukov GV, et al. A landscape of driver mutations in melanoma. Cell. 2012; 150:251–263. [PubMed: 22817889]

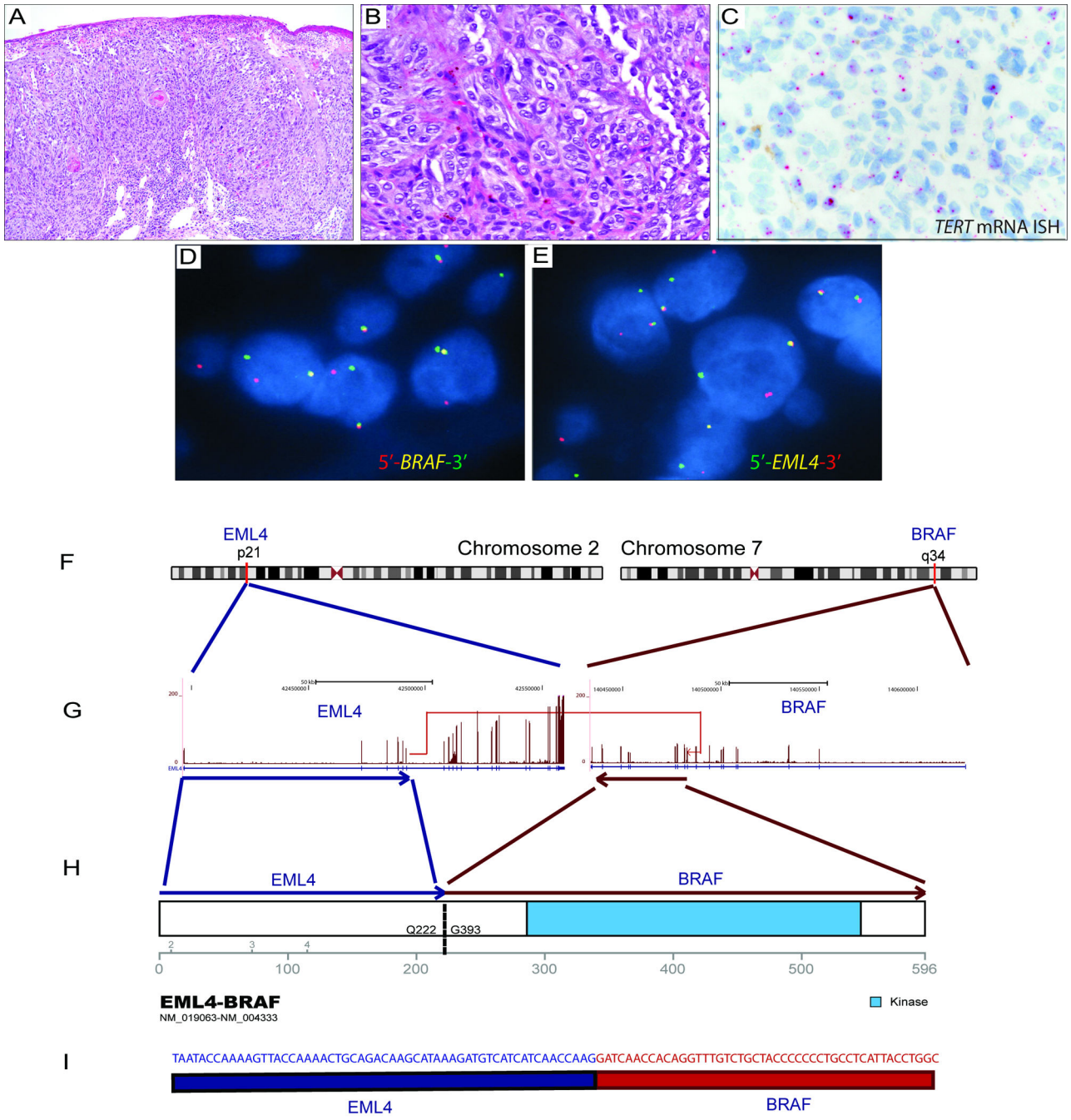

Figure 1. Spitzoid melanoma with the *EML4–BRAF* fusion transcript

Analysis of a tumor sample from a 14 year-old male (*patient 1*) with a 1.3-mm-thick spitzoid melanoma with microscopic sentinel lymph node metastasis at diagnosis and death as a result of disseminated disease in 18 months. (A, B) H&E photomicrographs (10× and 40×) of the primary tumor show compound proliferation of epithelioid and spindle-shaped spitzoid melanocytes arranged in confluent junctional nests with ulceration. (C) *TERT* mRNA ISH shows bright intracellular signals in melanocytes in this *TERT* promoter mutant melanoma. (D, E) Break-apart FISH shows splits of the red and green signals, which is

consistent with the rearrangement of *BRAF* and *EML4*, respectively. (F) Schematic figure depicting the reciprocal translocation between 2p21 and 7q34, resulting in the chimeric products *EML4–BRAF* and *BRAF–EML4.* (G) The in-frame fusion transcript produced by joining exon 6 of *EML4* (NM_019063, chr2:42491872) to exon 10 of *BRAF* (NM_004333, chr7:140482957). (H) The fusion transcript results in a 596-amino-acid chimeric protein containing the intact kinase domain of BRAF. (I) The RNA transcript contig shows the fusion breakpoint in the *EML4–BRAF* chimeric gene.

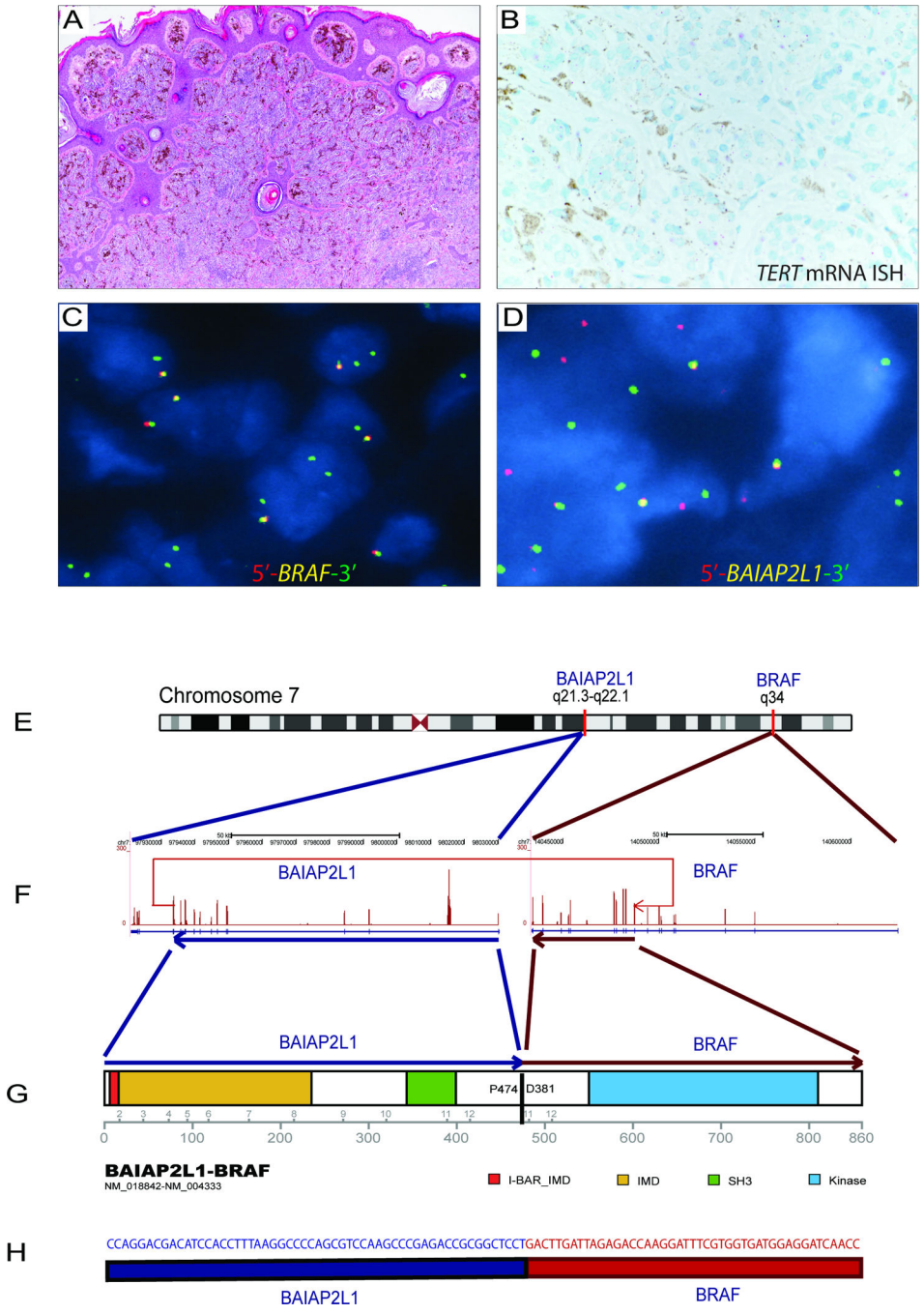

Figure 2. Spitzoid neoplasm with the *BAIAP2L1–BRAF* fusion transcript

Analysis of a tumor sample from a 4-year-old African-American female (*patient 2*) with a 7.8-mm-thick spitzoid melanocytic proliferation on her thigh, sentinel lymph node metastasis at diagnosis, and no evidence of disease at 53 months of follow-up. (A) H&E photomicrograph (4×) showing a dome-shaped proliferation of vertically oriented fascicles of spindled melanocytes throughout the reticular dermis. (B) *TERT* mRNA ISH shows no detectable intracellular signals beyond the background expression in this wild-type *TERT* promoter melanocytic tumor. (C) Break-apart FISH shows the rearrangement of *BRAF* with

loss of the 5 end (red signal), consistent with a complex translocation. (D) Break-apart FISH for *BAIAP2L1* shows splits of the red and green signals. (E) Schematic representation of the *BAIAP2L1–BRAF* fusion, showing that the fusion occurred by tandem duplication at 7q21.3–7q34. (F) The fusion transcript is formed by joining exon 12 of *BAIAP2L1* (NM_018842, chr7:97933507) to exon 9 of *BRAF* (NM_004333, chr7:140487384). (G) The fusion product is an 860-amino-acid chimeric protein containing the entire kinase domain of BRAF. (H) The RNA transcript contig shows the fusion breakpoint in the chimeric *BAIAP2L1-BRAF* transcript.

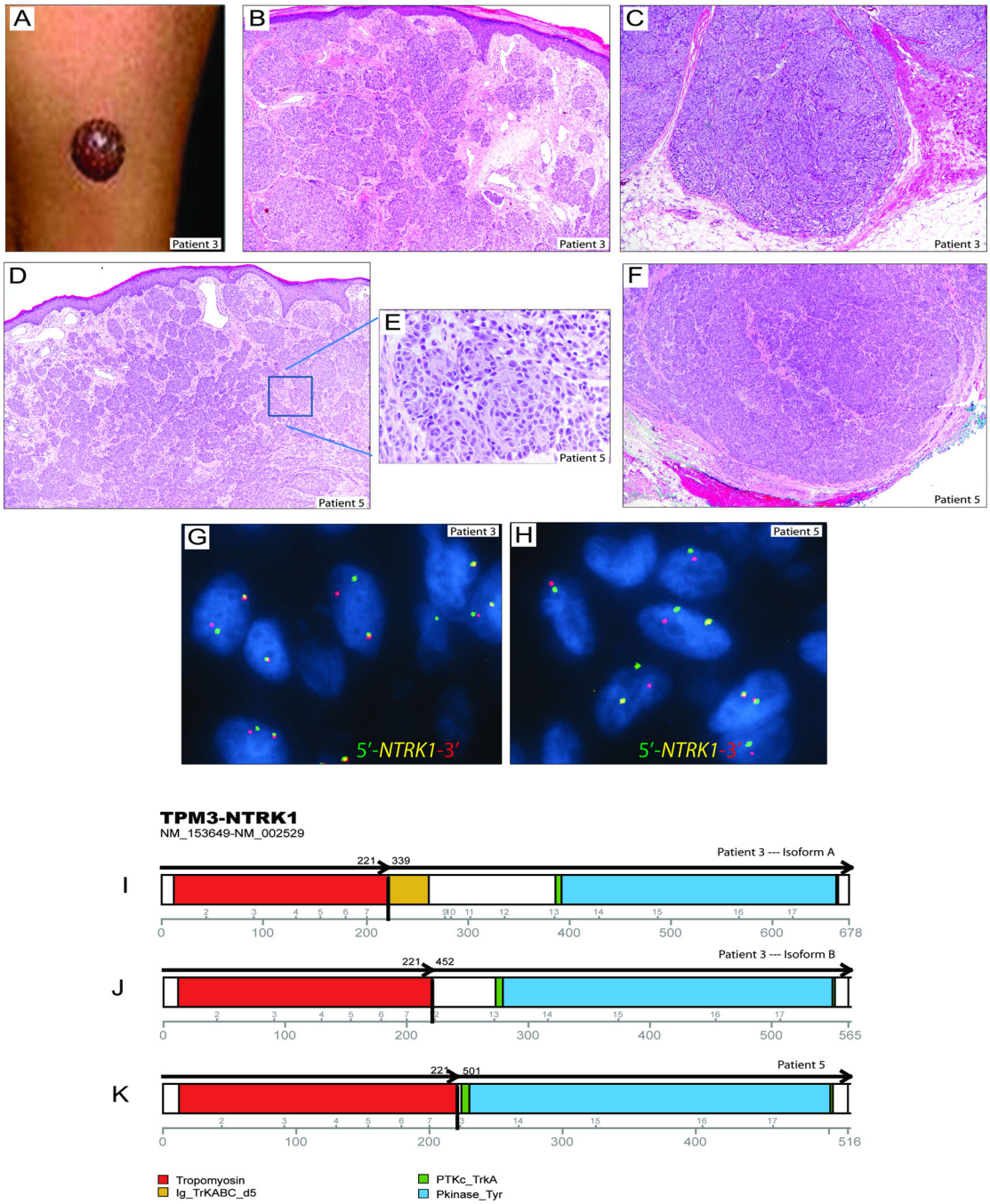

Figure 3. Multiple isoforms of the *TPM3–NTRK1* fusion transcripts in 2 spitzoid melanocytic tumors

(A) Photograph of a 2-year-old boy (*patient 3*) with an amelanotic exophytic nodule on the thigh, which was clinically thought to be a pyogenic granuloma. (B) H&E photomicrograph (4×) of the upper part of the lesion shows fascicles of spindled and epithelioid melanocytes arranged in whorls and nests with edema of the papillary dermis with telangiectasia. There were lymphovascular invasion and focal necrosis (not shown). (C) H&E photomicrograph (4×) of the bottom part of the lesion shows dumbbell-shaped configuration and deep extension into the subcutaneous fat. (D and F) H&E photomicrographs (4×) of the top and

bottom portions of a lesion on the ear of a 6-year-old female (*patient 5*) showing nests of polygonal shaped epithelioid melanocytes at high magnification (inset in E) that extend throughout the dermis and far into the basal line of resection margin in subcutis. (G, H) Break-apart FISH for *NTRK1* shows split signals in both spitzoid tumors. (I–K) The *NTRK1* fusion gene encoded 2 variant TPM3–NTRK1 isoforms in *patient 3* and a third isoform in *patient 5*. All isoforms retained the intact tyrosine kinase domain of NTRK1.

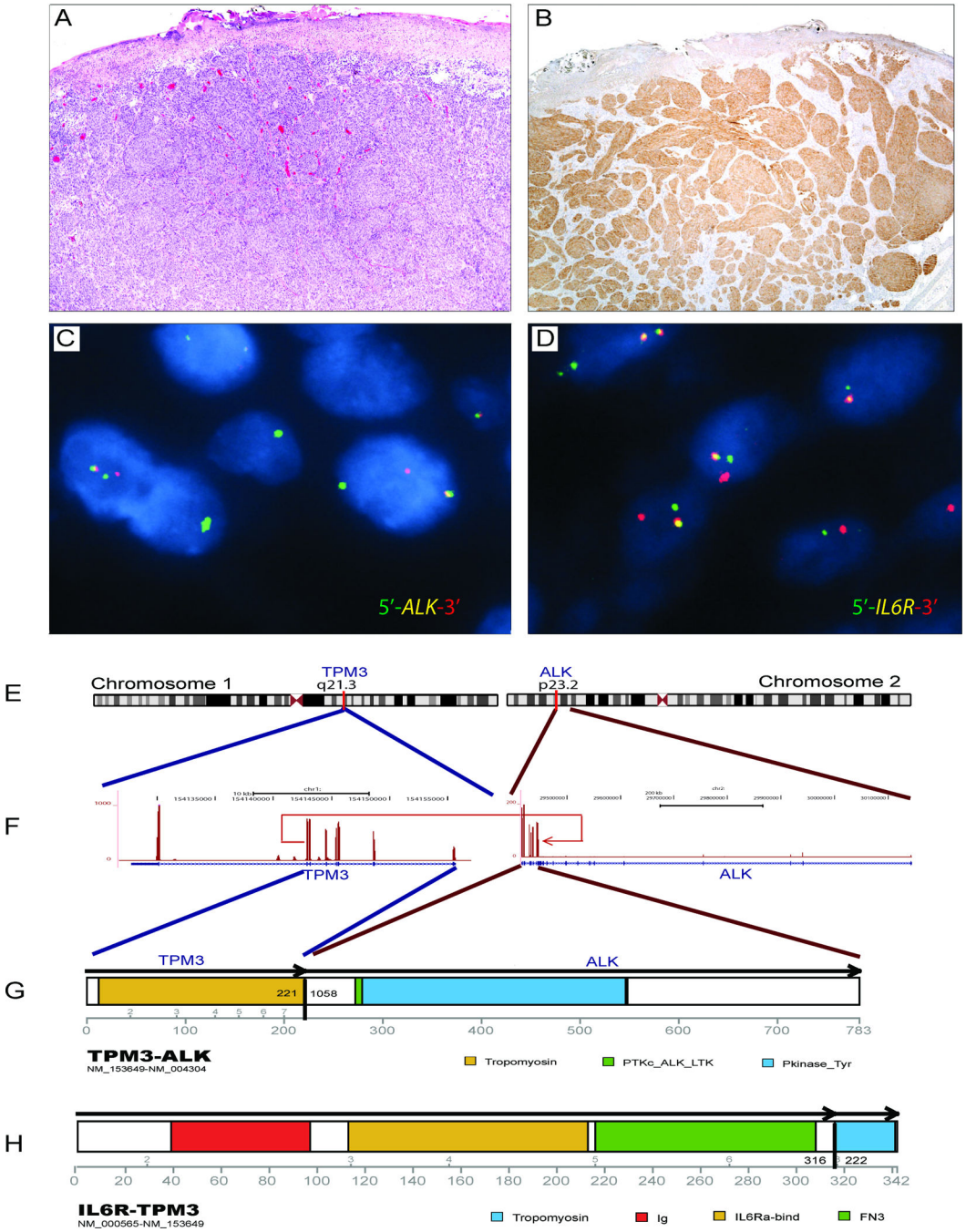

Figure 4. Complex genomic rearrangements involving *ALK, TPM3*, and *IL6R*

Spitzoid melanocytic neoplasm in the calf of a 13-year-old female (*patient 4*). (A) H&E photomicrograph showing nests of spindled melanocytes with ulceration. (B) ALK immunoreactivity highlights a fascicular architecture in the dermis. (C, D) Break-apart FISH for *ALK* and *IL6R* confirms rearrangements in the respective genes. (E–H) Schematic of the *TPM3–ALK* fusion gene. The first 222 amino acids of TPM3 are fused to the C terminus of ALK, incorporating the intact tyrosine kinase domain of ALK. The remaining TPM3 protein

is fused to the IL6R protein. The identification of multiple fusions involving *TPM3* suggests a complex translocation event.

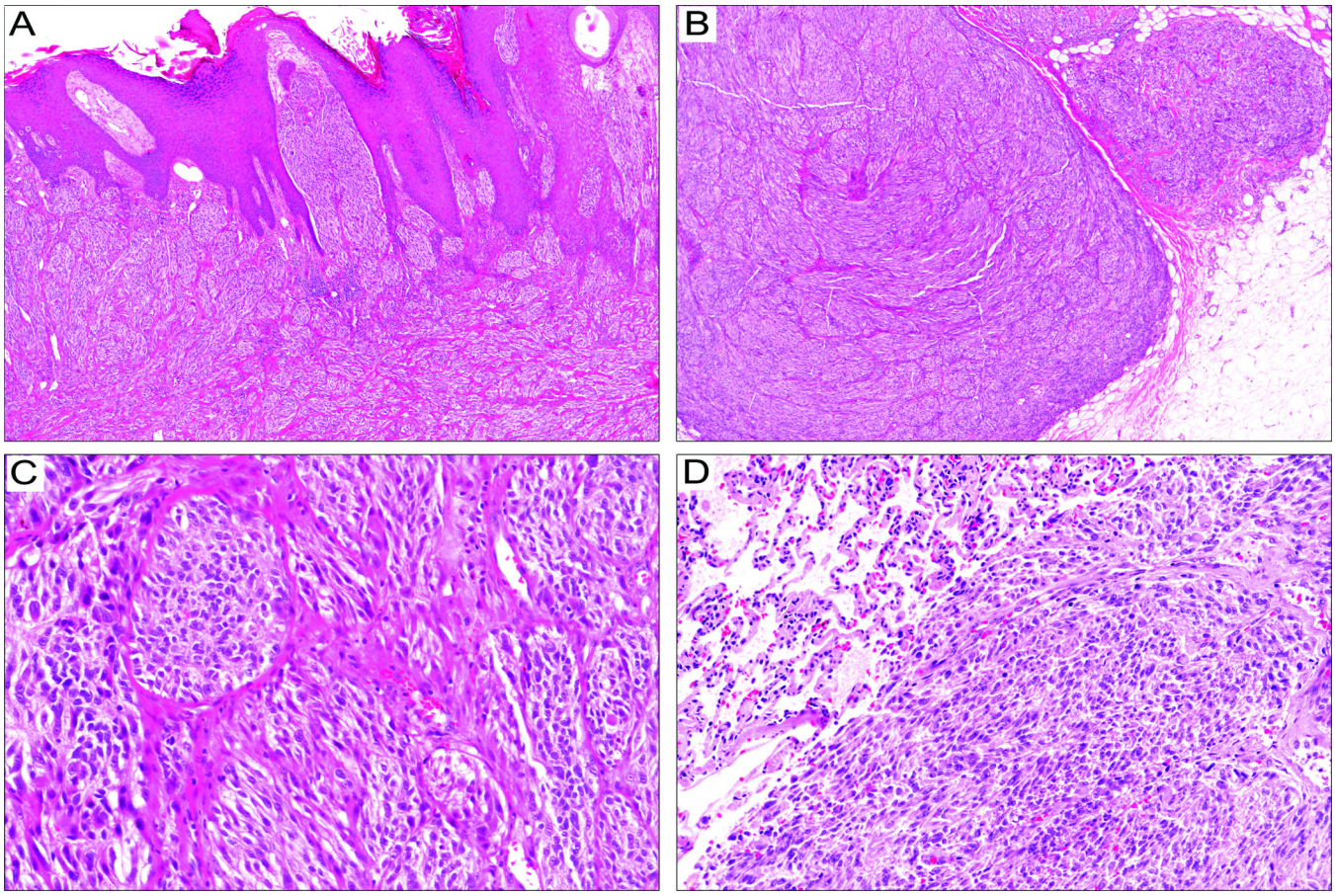

Figure 5. Spitzoid melanoma with a *TERT* promoter mutation and fatal outcome

An 11-year-old girl (*patient 7*) presented with a lesion on her thigh with an initial histologic diagnosis of a Spitz nevus, bulky nodal metastasis in 6 months, and disseminated disease and death 24 months after diagnosis. (A) Scanning magnification shows closely packed nests of spindle-shaped melanocytes with pseudoepitheliomatous hyperplasia and telangiectasia in the upper dermis. (B) The lower half of the lesion shows dense cellularity, sheet-like arrangement, and deep extension into subcutis. (C) Intermediate magnification shows confluent fascicles of spindle shaped melanocytes. (D) Metastatic lung nodule composed of morphologically similar spindled melanocytes.

Table 1

Clinical, pathological, and genomic characteristics for the seven patients with spitzoid melanoma or biologically indeterminate spitzoid tumors

Case	Patient 1	Patient 2	Patient 3	Patient 4	Patient 5	Patient 6	Patient 7
Age	14y 0m	4y 2m	2y	13y	6y	2y	11y 2m
Gender	M	F	M	F	F	M	F
Primary site	back	leg	thigh	calf	ear	knee	thigh
Thickness(mm)	1.3	7.8	8.2	4	9.1	13.3	7
Ulcer	Y	N	N	Y	N	Y	Y
Mitotic rate	5	5	8	3	7	1	7
Diameter(mm)	11	10	17	9	11	15	12
SLN metastasis	Y	Y	Y	N	Y (mac)	NP	Y (mac)
Outcome	DOD 18m	NED 53m	NED 20m	NED 6m	NED 18m	NED 72m	DOD 24m
Fusion transcript by RNA-Seq	*EML4-BRAF, BRAF-EML4*	*BAIAP2L1-BRAF, ARID1B-SNX9*	*TPM3-NTRK1, PTPRZ1-NFAM1*	*TPM3-ALK, IL6R-TPM3, IL6* Intergenic	*TPM3-NTRK1*	None	Failed
BRAF mutation	Negative	Negative	Negative	Negative	Negative	Negative	Negative
NRAS mutation	Negative	Negative	Negative	Negative	Negative	Negative	Negative
TERT promoter mutation	−124C>T	Negative	Negative	Negative	Negative	Negative	−124C>T
TERT mRNA ISH	Positive	Negative	Negative	Negative	Negative	Negative	Failed

Abbreviations: M: male; F: female; y: years old; m: months; SLN: sentinel lymph node; Y: yes; mac: macrometastasis; NP: not performed; DOD: dead of disease; NED: no evidence of disease; ISH: in situ hybridization.